Deep-Sea Research Part I 141 (2018) 1–10

Contents lists available at ScienceDirect

Deep-Sea Research Part I

journal homepage: www.elsevier.com/locate/dsri

The subsurface circulation of the Iceland Sea observed with RAFOS floats

M. Femke de Jong[a,*], Henrik Søiland[b], Amy S. Bower[c], Heather H. Furey[c]

[a] Royal Netherlands Institute for Sea Research and Utrecht University, Texel, The Netherlands
[b] Institute of Marine Research, Bergen, Norway
[c] Woods Hole Oceanographic Institution, Woods Hole, MA, USA

ABSTRACT

The pathways of dense waters located above the sill depth of Denmark Strait were investigated in the Iceland Sea using 52 acoustically tracked RAFOS floats. These floats were deployed in summer 2013 and 2014, with a target depth of 500 m, resulting in a total of 40.9 float-years of track data covering the Iceland Sea basin. In the interior Iceland Sea basin, the float tracks showed a double gyre circulation, out of which floats eventually escaped towards the Norwegian Sea in the East Icelandic Current, with some appearing to be en route to the Faroe Bank Channel. Four floats exited through Denmark Strait and surfaced in the Labrador and Irminger Seas. Four other floats deployed west of the Kolbeinsey Ridge at 70°N show the connection between the East Greenland Current and the East Icelandic Current. Floats deployed east of the Kolbeinsey Ridge along the Icelandic slope were captured in a region with no clear main flow. Eddy motions, mainly small scale (radii of 0.5–3 km), are seen throughout the Iceland Sea. Several floats were grounded on the Icelandic slope both east and west of the Kolbeinsey Ridge due to upslope currents, which created a rim of cold water along the slope. While this water was indicative of the presence of the North Icelandic Jet, no connection between the eastern Iceland Sea and Denmark Strait sill was found. Our investigation of wind stress curl fields from atmospheric reanalysis data suggests that high wind stress curl conditions may have been unfavorable for a westward connection by the North Icelandic Jet at the time of the float observations.

1. Introduction

The Iceland Sea or Iceland Plateau is located between Iceland, east Greenland and Jan Mayen (Fig. 1). This basin, although relatively small, is thought to play an important role in the exchange between the North Atlantic and the Nordic Seas, which includes the Greenland Sea to the north and the Norwegian Sea to the east. The surface currents have been relatively well described early on (Helland-Hansen and Nansen, 1909). Warm and saline water enters the Iceland Sea from the North Atlantic in the North Icelandic Irminger Current (NIIC). The East Greenland Current (EGC) advects fresh, cold water southward to the North Atlantic along the Greenland shelf. The East Icelandic Current (EIC) diverges off the East Greenland shelf eastward to the Norwegian Sea (Macrander et al., 2014).

At deeper levels, the EGC advects a core of relatively warm and saline water. This water, named return Atlantic Water by Mauritzen (1996) and sometimes called recirculated Atlantic Water (Jeansson et al., 2008), first entered the Artic Mediterranean across the Iceland-Faroe Ridge in the Norwegian Atlantic Current and is modified (e.g. cooled and freshened) along its cyclonic transit through the Nordic Sea and the Arctic basin. Mauritzen (1996) proposed that the return Atlantic Water (RAW), which is shallow enough to overflow the sill (650 m) of Denmark Strait into the Irminger Basin, is the main contributor to Denmark Strait Overflow Water.

Earlier studies by Swift et al. (1980) proposed a more local source for the dense overflow waters. They proposed that the overflow water shared properties with upper Arctic Intermediate Water and that this water mass was formed by local cooling in the Iceland Sea. Later Smethie and Swift (1989) adjusted this Iceland Sea source to include a secondary Greenland Sea source to account for the older age of the overflow water derived from isotope ratio measurements. Since water mass transformation in winter has high interannual variability, these proposed sources did not account for the nearly constant outflow at Denmark Strait. Therefore Mauritzen (1996) proposed the return Atlantic Water, whose inflow from the Atlantic into the Norwegian Seas is more stable, as a source. Rudels et al. (2002a,2002b) further elaborated on this circulation scheme, with a main source in the EGC but allowing for exchange with intermediate waters in the Greenland and Iceland Sea gyres.

An Iceland Sea source came back in focus as a result of the work of Jónsson (1999) with current meter data from the northeast part of Denmark Strait showing southwestward flow. Jónsson and Valdimarsson (2004) identified a jet flowing westward towards Denmark Strait along the northern continental slope of Iceland. A more extensive hydrographic study by Våge et al. (2011) coined the name North Icelandic Jet (NIJ) for this feature. Their sections showed that the NIJ is only marginally present east of 15°W and becomes progressively stronger towards Denmark Strait. Results from an idealized model

* Corresponding author.
E-mail address: femke.de.jong@nioz.nl (M.F. de Jong).

https://doi.org/10.1016/j.dsr.2018.07.008
Received 5 October 2017; Received in revised form 29 June 2018; Accepted 14 July 2018
Available online 17 July 2018
0967-0637/

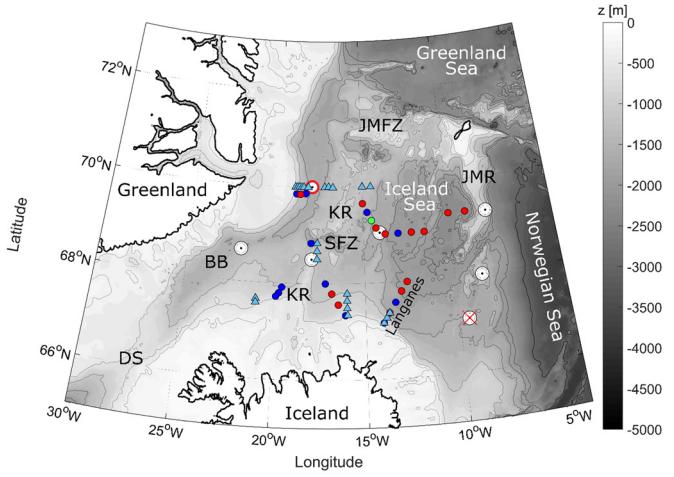

Fig. 1. Bathymetry of the Iceland Sea. Isobaths are drawn at 500, 1000, 1500, 1800 and 2000 m depth, shading at 100 m interval. Floats were deployed in July 2013 (circles) with mission lengths of 160 days (green), 280 days (dark blue) and 650 days (red). Floats deployed in July 2014 (triangles) all had 320 day missions (light blue). Note that a blue and red circle are plotted underneath the first three triangles on the inshore end of the Langanes section. Six sound sources (white concentric circles) ensonified the basin. The sound source in the southeastern basin (red cross) was replaced by a sound source in the east Greenland channel (red outer circle) in the second year. The acronyms denoting bathymetric features are: Denmark Strait (DS), Blosseville Basin (BB), Kolbeinsey Ridge (KR), Spar Fracture Zone (SFZ), Jan Mayen Fracture Zone (JMFZ) and the Jan Mayen Ridge (JMR). (For interpretation of the references to color in this figure legend, the reader is referred to the web version of this article.)

(Våge et al., 2011) suggested that downwelling near the slope, which compensates buoyancy loss (through eddies and surface fluxes) of the NIIC, can explain the existence of the NIJ. Logemann et al. (2013a,2013b) suggest that the baroclinic pressure gradient of the Arctic Front, located between the warm NIIC and the cold Arctic water to the north, forces the NIJ. Several studies (Rudels et al., 2003; Köhl et al., 2007) suggested that the overflow may (partially) switch between the Iceland Sea and the EGC sources. The variability in the model study by Köhl et al. (2007) was controlled by changes in reservoir height and barotropic transport changes associated with the wind stress curl around Iceland.

Rudels et al. (2002a,2002b) noticed that the flow in the channel just upstream of Denmark Strait is quite complex. They remarked that the core of the EGC separated from the slope and moves toward the middle of the channel. In the model of Köhl et al. (2007) the EGC appears to cross over completely to the eastern side of the channel. Harden et al. (2016) suggest that the EGC splits into two branches, based on a year-long record from a mooring array across the channel just upstream of Denmark Strait. They propose that the overflow consists of three contributions, the EGC, the separated EGC and the NIJ. In this partitioning the EGC is the largest contributor in volume and variability and the separated EGC and NIJ show compensating variability.

All of these studies depend on Eulerian measurements, being either hydrographic sections and/or mooring data. However, while these Eulerian measurements are very useful to get transport estimates of DSOW (Jochumsen et al., 2017) they do not conclusively show the connectivity between the different sections. While GPS-tracked surface drifters are suitable to study the (near-)surface flow, subsurface acoustically-tracked RAFOS floats are employed to elucidate the subsurface flow. Because these floats do not need to surface to fix a position, they can better track the dense water pathways. This is especially important in the Iceland Sea because of the complex bathymetry and the eastward directed East Icelandic Current, which is found above and north of the westward directed NIJ. Here we report on results from a recent deployment of 52 RAFOS floats in the Iceland Sea. The trajectories of the floats give direct insight into the subsurface circulation of the Iceland Sea and the pathways of dense water toward Denmark Strait. The paper is organized as follows: Section 2 describes the RAFOS experiment as well as additional data sets used in this study. In Section 3, we present the subsurface tracks obtained from the RAFOS floats. In Section 4, we discuss the results in relation to previous observations as well as with regard to the atmospheric forcing conditions during the experiment.

2. Data

2.1. RAFOS floats and shipboard data

Acoustically tracked subsurface RAFOS floats (Rossby et al., 1986) have been used in several studies to investigate ocean circulation in a Lagrangian sense, but there have been relatively few deployments in the Nordic Seas (Søiland et al., 2008; Rossby et al., 2009). Data from the RAFOS floats reported here are signals, emitted once daily, from six sound sources moored in the Iceland Sea from July 2013 through July 2015. The floats were able to hear the sound source signals up to 600 km away. Position accuracy is affected by float and source clock accuracy and variations in the sound velocity field between the float and sound sources. After correction for clock drift we estimate the final float position accuracy to be about two kilometers. However, the relative data-point-to-data-point positions within the same trajectory are much more accurate, since all three factors are substantially mitigated within the same instrument and nearby sampling interval. Some topographic shadowing occurred towards the Denmark Strait sill, where the channel narrows. An additional sound source was therefore added to the tracking array in the western part of the Iceland Sea in July 2014.

The RAFOS floats were built by Seascan, Inc. in Falmouth, Massachusetts and ballasted in the high-pressure tanks at the University of Rhode Island (URI) Graduate School of Oceanography and Woods Hole Oceanographic Institution (WHOI). The floats were ballasted for 500 dbar, to target the North Icelandic Jet, the East Icelandic Current, and other mid-depth currents of the Iceland Sea. Ballasting accuracy is to within one gram, which is roughly equivalent to 35 m depth. In practice, some of the floats settled deep, usually between 600 and 800 dbar. This was due to a new construction material used in the insulator component of the drop-weight assembly, Ultra-High Density Plastic (UHDP). The UHDP has a different thermal expansion coefficient (TEC) than the previous insulator component, and this was not accounted for in the ballasting calculations. The incorrect TEC caused the floats to be overballasted, and this has been since corrected in the ballasting equations. The calculation of the additional ballast weight to be added to a float is dependent on the target deployment pressure and ambient water conditions, including temperature. The incorrect TEC mainly affected the subset of 12 floats ballasted in the WHOI warm (20 °C) tank, as the 4 °C water in the URI tank is closer to temperatures in the Iceland Sea. In subsequent RAFOS programs, the UHDP material has been removed from the float dropweight assembly.

The floats record pressure and temperature, as well as times-of-arrival of the acoustic signals generated by the sound sources. The pressure and temperature were derived from a module manufactured and calibrated by Seascan, Inc., which utilized a thermistor as the temperature sensor and a Druck pressure sensor. Temperature accuracy is ± 0.005 °C and pressure, ± 5 dbar. The floats are passive drifters, and did not surface until mission end, when the dropweight was separated from the float by a burnwire, and the float, now positively buoyant, surfaced and transmitted its data using Short Burst Data technology via the Iridium network. Final positions are determined at the surface by the GPS antenna on the floats, which ensures accuracy of the underwater float trajectory at this position.

The RAFOS floats were deployed in two batches, each containing 26 floats. The first batch, deployed in July 2013, consisted of 13 (12) floats

Table 1
Float information: Serial number ID, mission length, initial pressure [dbar], date [dd-mm-yyyy] and position of deployment [decimal degrees °N and °W], date and position of surface, remarks. Floats that did not surface are marked as "DNS". Floats that were grounded on the Iceland shelf are marked with "ground", two floats (indicated with a *) have some free floating trajectories after being grounded. Surface locations away from the Iceland Sea; near the Faroe Bank Channel (FBC), in the Irminger Sea (IS) and Labrador Sea (LS), are also marked. Floats without remarks surfaced within the Iceland Sea. One of the FBC floats has no track due to a clock error (ce).

Float info			Deployment			Surface			
ID	Mission [days]	Pres [dbar]	Date [dd-mm-yyyy]	Lat [°N]	Lon [°W]	Date [dd-mm-yyyy]	Lat [°N]	Lon [°W]	remarks
1200	280	589	24-07-2013	68.84	18.03	30-04-2014	67.51	25.83	
1201	280	570	23-07-2013	67.34	16.11	29-04-2014	67.27	17.58	
1202	280		25-07-2013	67.72	19.91				DNS
1203	650	565	26-07-2013	69.65	15.01	07-05-2015	67.90	9.81	
1205	650	579	27-07-2013	69.34	10.01	08-05-2015	68.60	13.64	
1212	280	581	23-07-2013	67.58	13.37	29-04-2014	68.17	7.15	
1213	650	585	23-07-2013	67.81	13.02	04-05-2015	63.44	4.38	FBC, ce
1214	650	596	23-07-2013	68.00	12.68	04-05-2015	70.73	11.13	
1257	280	767	23-07-2013	67.17	14.05	29-04-2014	66.36	12.07	Ground
1258	650	751	23-07-2013	67.37	13.72	04-05-2015	62.16	2.83	FBC
1259	280	843	24-07-2013	67.91	19.60	30-04-2014	67.92	19.60	Ground
1260	280	789	25-07-2013	69.85	18.93	01-05-2014	67.47	22.05	Ground
1261	280	744	24-07-2013	68.00	17.20	30-04-2014	66.57	12.55	
1262	650		25-07-2013	69.85	18.69				DNS
1263	650	735	27-07-2013	69.00	11.49	08-05-2015	70.27	16.19	
1264	650	740	27-07-2013	69.33	9.03	08-05-2015	69.30	10.26	
1269	650	781	27-07-2013	69.01	12.24	08-05-2015	66.37	8.03	
1270	280	761	26-07-2013	69.01	13.01	02-05-2014	68.78	12.82	
1275	280		26-07-2013	69.47	14.76				DNS
1276	160	764	26-07-2013	69.29	14.51	30-12-2013	68.54	13.95	
1277	650	690	26-07-2013	69.14	14.27	07-05-2015	65.48	9.62	
1278	650	712	26-07-2013	69.00	13.75	06-05-2015	67.74	9.57	
1279	280	704	24-07-2013	67.80	19.76	30-04-2014	67.36	23.44	Ground
1280	280	706	26-07-2013	69.86	18.37	02-05-2014	67.63	20.21	Ground
1281	650	780	24-07-2013	67.56	16.49	05-05-2015	65.51	8.04	Ground*
1282	650	743	24-07-2013	67.79	16.85	05-05-2015	67.75	16.08	Ground
1206	320		11-07-2014	67.58	21.00				DNS
1207	320		11-07-2014	67.58	21.00				DNS
1208	320	542	12-07-2014	70.00	19.00	29-05-2015	63.13	54.35	LS
1209	320	542	12-07-2014	70.00	19.00	29-05-2015	62.56	58.66	LS
1210	320	508	09-07-2014	67.17	14.05	28-05-2015	67.72	14.72	
1211	320	539	10-07-2014	67.34	15.98	26-05-2015	64.46	9.27	Ground
1287	320	592	13-07-2014	69.99	16.76	29-05-2015	66.88	11.95	
1288	320	572	13-07-2014	70.00	15.0	29-05-2015	66.88	11.02	
1289	320	610	11-07-2014	68.50	17.68	27-05-2015	65.84	10.49	
1290	320		11-07-2014	68.67	17.67				DNS
1291	320	591	13-07-2014	69.99	18.62	29-05-2015	66.60	9.52	
1292	320	1018	13-07-2014	70.00	18.50	15-07-2014	69.83	18.53	Bail out
1293	320	595	13-07-2014	70.00	17.01	29-05-2015	66.25	10.93	
1294	320	579	13-07-2014	69.99	16.76	29-05-2015	67.92	15.84	
1295	320	613	10-07-2014	67.64	16.01	26-05-2015	67.49	18.29	Ground
1296	320	588	11-07-2014	68.83	17.67	27-05-2015	65.54	8.17	
1297	320	569	13-07-2014	70.00	18.88	29-05-2015	64.68	34.39	IS
1298	320	630	13-07-2014	70.00	18.75	29-05-2015	67.35	23.57	Ground
1299	320	564	11-07-2014	67.66	21.00	27-05-2015	67.54	23.25	Ground
1300	320		11-07-2014	67.66	21.00				DNS
1301	320	576	13-07-2014	69.99	18.24	29-05-2015	59.80	55.18	LS
1302	320	593	13-07-2014	70.00	17.25	29-05-2015	67.87	15.21	
1303	320	599	10-07-2014	67.27	13.88	26-05-2015	65.27	9.81	Ground*
1304	320	584	10-07-2014	67.37	13.72	26-05-2015	67.18	18.44	Ground
1305	320	592	10-07-2014	67.49	16.00	26-05-2015	67.90	18.31	Ground
1306	320	575	10-07-2014	67.79	16.00	26-05-2015	67.68	15.18	

with 650-day (280-day) missions and one float with a short 160-day mission for test purposes. In the second batch, deployed in July 2014, all 26 floats had 320-day missions. Fig. 1 shows the deployment positions of all floats. Ten floats from the first batch of floats were deployed in the deep region of the central Iceland Sea. These were mostly long-mission floats, because of the expected low velocities in this part of the basin. The remainder of the floats was deployed on a section perpendicular to the East Greenland slope at approximately 70°N and on three sections crossing the continental slope north of Iceland. The majority of these floats were deployed east of the Kolbeinsey Ridge (KR) in order to study the possible pathway of the NIJ to Denmark Strait. The second year float deployments focused on the 70°N section, the Icelandic slope and the Spar Fracture Zone (Fig. 1), a passageway in the Kolbeinsey Ridge at approx. 69°N. Float mission details are included in Table 1. Usable tracks were derived for a total of 44 floats, with a total of 40.9 float-years of track data.

The cause of float failures (floats that did not surface or no-shows) among those deployed on the northwestern slope of Iceland and the KR is most likely due to rough interaction with the bottom. We recovered one float in 2015 that had been in contact with the bottom and the glass and endplate had been scratched, indicating contact with a rocky (volcanic) bottom. It is possible that the dropweight may be ripped off in contact with the bottom. In fact, the early surfacing of one float that was sitting on the bottom was caused by the drop weight ripped off as it was in contact with the bottom. Also, the fraction of no-shows from the floats deployed east of the KR is much smaller, thus indicating that bottom contact may be the cause of many no-shows.

CTD (conductivity, temperature, depth) stations were taken at nearly all float deployment positions during the 2013 and 2014 cruises. The hydrographic profiles allow us to see where the floats initially are in T,S-space. All floats were deployed in water with $\sigma_\theta > 28.0\,\mathrm{kg\,m^{-3}}$ and were therefore considered to be embedded in overflow water. An example of the float deployment locations and depths on an hydrographic section taken on the deployment cruise is shown in Fig. 2.

2.2. Wavelet analysis

The RAFOS floats were at times embedded in flow that exhibited looping motion indicative of coherent eddies capable of trapping and transporting water (and floats). To quantify these trajectory motions we utilized Matlab-based wavelet analysis software provided by J. Lilly (http://www.jmlilly.net/jmlsoft.html). This methodology has been documented in a series of papers (Lilly and Olhede, 2009a, 2009b, 2010a, 2010b, 2012) which were based on a prototype study by Lilly and Gascard (2006). The analysis method is performed by finding the "best fit" of the float trajectory data to a mathematical model for the displacement signal of a particle orbiting the center of an eddy, using a procedure known as wavelet ridge analysis. By using this analytical method, we were able to objectively identify cyclonic and anticyclonic coherent eddies in the data set, along with statistics on their kinematic properties such as rotation period, diameter, azimuthal velocity, and Rossby number. Because of edge effects, we discarded output equal to one rotation period of the eddy at both the start and end of the eddy segment, as described in Bower et al. (2013). In practice, if a float was in an eddy for three complete loops, the values of radius, velocity, and Ro are based only on the mean value of the middle loop.

2.3. Additional data

Atmospheric data at 0.25° resolution were obtained from the ERA Interim reanalysis. Daily fields of radiative and turbulent heat fluxes as well as 10 m eastward (u) and northward (v) wind components from January 1979 to September 2016 were downloaded from apps.ecmwf.int/datasets/data/interim-full-daily/. Wind stress curl fields were calculated from the 10 m u and v wind fields following Gill (1982).

Argo trajectories from the Iceland Sea were obtained from http://www.argodatamgt.org/Access-to-data/Argo-data-selection. A total of 21 Argo floats were deployed in the Iceland Sea between 2005 and 2017. The typical parking depth of the Argo floats in the Iceland Sea is 1000 m, therefore the 10-day Argo displacement trajectories provide additional information about the circulation in the deeper parts of the basin.

3. Results

The RAFOS float tracks cover the area of the Iceland Sea south of

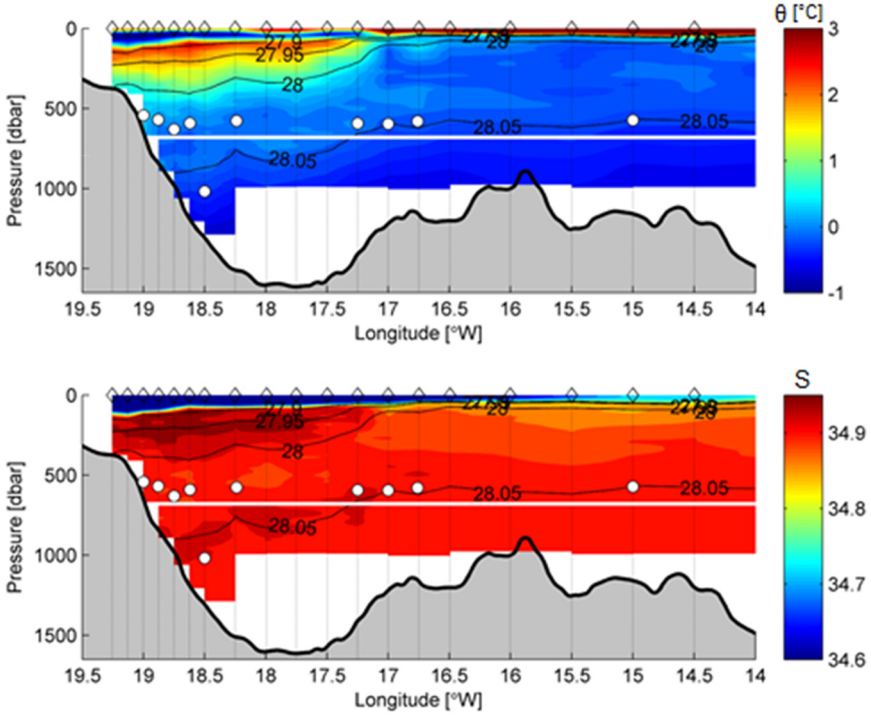

Fig. 2. CTD section in the east Greenland channel at approx. 70°N surveyed in July 2014. Shown are potential temperature (top panel) and salinity (bottom panel) along with isopycnals (black lines). Station positions are indicated with dashed vertical lines. July 2014 RAFOS release positions and depths from Table 1 are indicated with white circles. The sill depth of Denmark Strait is indicated with the horizontal white line. Note that the RF1292 is located significantly deeper than the other floats. This (presumably leaky) float continued to sink and bailed out shortly after.

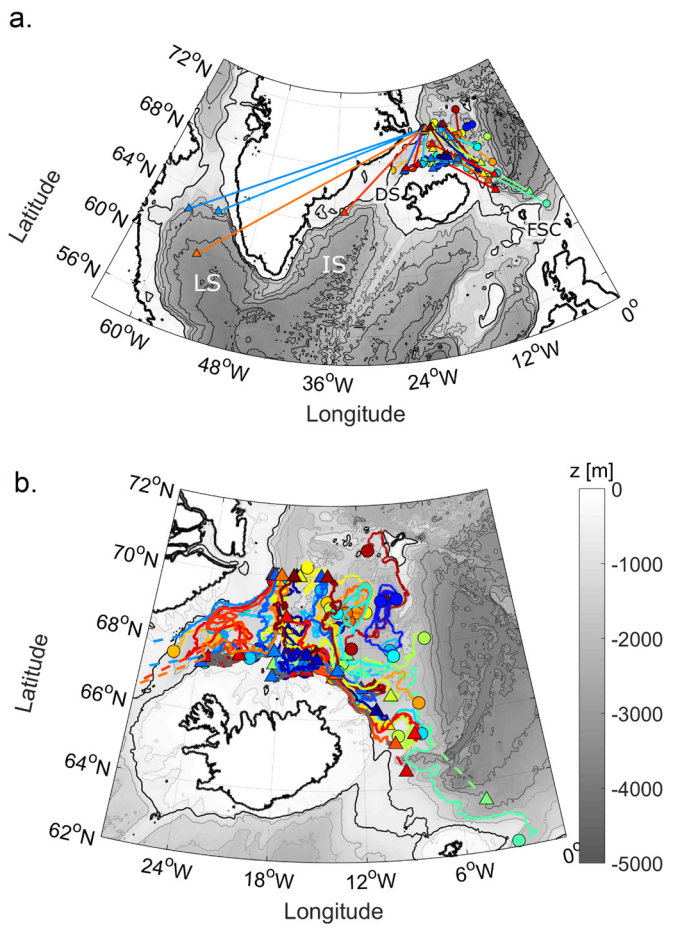

Fig. 3. Displacement vectors between deployment and surface positions of (a.) all floats and (b.) trajectories of all floats within the Iceland Sea. First year deployments are indicated with circles and second year deployments with triangles. Dashed lines are drawn from last known subsurface position to the surface position. Grounded position are indicated in gray. The 500 m isobaths is indicated in black. Acronyms used for bathymetry are: LS Labrador Sea; IS Irminger Sea; DS Denmark Strait and FCS Faroe Shetland Channel.

70°N (Fig. 3). During the two-year period, most of the floats did not leave the Iceland Sea before the end of their programmed mission, whereas about 13% (six floats) escaped by two main routes; four floats crossed the Denmark Strait sill and surfaced in the Irminger (RF1297) and Labrador Seas (RF1208, 1209 and 1301) and two floats surfaced near the Faroe Bank Channel overflow (RF1213 and 1258; Fig. 3 & Table 1). Floats deployed in the interior Iceland Sea, east of the KR, recirculated within the deep basin and eventually escaped south of the Jan Mayen Ridge towards the Norwegian Sea. Floats deployed west of the KR show the southwestward flow of the East Greenland Current as well as a connection to the interior Iceland Sea. Overall, current speeds were low, averaging about 3.8 with a standard deviation of 3.6 cm s^{-1}, except for two regions. Higher velocities were measured in off the Greenland slope in the southwestward East Greenland Current and in the southeastward direction along a particularly steep part of the northeastern Icelandic slope, between 10°W and 15°W. In the following paragraphs we will discuss the float tracks in more detail.

3.1. The circulation in the interior Iceland Sea

Latarius and Quadfasel (2016) noted the large residence time of Argo floats in the Iceland Sea (2.1 year) compared to the other Norwegian Seas basins. The RAFOS floats show the circulation of the northeastern part of the Iceland Sea to be characterized by a double cyclonic gyre (Fig. 4). The two gyre cells seem to be defined by the bathymetry, which shows two separate depressions in the deepest part of the basin. The recirculation in this region was slow, with the floats in the easternmost cell moving at approx. 2.5 ± 1.5 cm s^{-1}. The double gyre circulation was also seen in Argo float displacements (Fig. 4), but because of their 1000 m park depth, the Argo floats were even more strongly confined to this deep part of the Iceland Sea. Voet et al. (2003) estimated gyre velocities between 1 and 1.5 cm s^{-1} at 1000 m depth based on Argo data. Many of the Argo floats showed several (up to five) circuits around these two bathymetric depressions. Of the 21 Argo floats, 11 eventually escaped the Iceland Sea to the Norwegian Sea through a gap in the Jan Mayen Ridge at 67°N. Two of these continued south to the Iceland Basin through the Faroe Bank Channel.

Several RAFOS floats followed the same path, although their shallower depth allowed them to escape the cyclonic cells at different locations. One float (RF1214) followed the Jan Mayen Ridge north into the Jan Mayen Fracture Zone. Float RF1263 traveled west and circulated around the equally complicated topography of the KR. However, most of the RAFOS floats deployed in the interior basin exited towards the Norwegian Sea. These floats were joined by several floats deployed east and west of the KR. On the east side, the float trajectories (RF1287 and 1288) deployed near the ridge followed the topography to the southwest, while exhibiting higher eddy activity. At the Spar Fracture Zone, the trajectories diverge from the topography and turn southeast. Four trajectories of floats deployed west of the Kolbeinsey Ridge (RFs 1291, 1292, 1294 and 1302) passed through Spar Fracture Zone and joined the southeastward flow of the East Icelandic Current. Notably, even one float (RF1291) deployed in the East Greenland Current proper follows this path, even though several floats (RFs 1297, 1298 and 1301) deployed nearby (partially) followed the EGC southward and remained west of the ridge.

3.2. Pathways near the Icelandic slope east of the Kolbeinsey Ridge

The southeastward directed trajectories described above converged on the northeastern Icelandic slope. On this particularly steep part of the bathymetry, the flow appeared to be nearly linear and flow speeds increased to a maximum of 48 cm s^{-1}. These instantaneous velocities fall within the highest range of velocities documented by Macrander et al. (2014), who analyzed current meters moored on the shelf in the Langanes section, suggesting that the off shelf flow is significantly faster. As the bathymetry widens further east, the floats slow down. One float (RF1277) recirculates around a shallow promontory located at 66.7°N and 10°W, while showing small scale coherent eddy motions (radius of 1–2 km and a period ~ 4 days) at the same time. Two floats (RFs 1213 and 1258) continue southeast along the Iceland Faroe Ridge. This pathway could potentially contribute to the Faroe Bank Channel overflow.

The wedge south of the Spar Fracture Zone, between the eastern flank of the Kolbeinsey Ridge at 18.5°W and the Icelandic slope at 13.5°W is a region with no clear mean flow in the float trajectories. (Fig. 5). This is somewhat surprising, since the (eight) floats were deployed in an attempt to capture the expected westward flow of the NIJ around the Kolbeinsey Ridge. None of these floats transited west through the Spar Fracture Zone. One float trajectory (RF1201) described an anti-cyclonic motion east of the ridge, with northward flow up to 68.25°N before turning southeast. Although the area is well covered by the trajectories, nearly all of them are showing non-coherent small scale motions in the inner near-shelf region and more coherent motions (described in Section 3d) on the eastern edge of this region, between 14° and 16.5°W. Eventually these floats either exit the region in the southeast or are stranded on the Iceland slope. The floats grounding around 18°W show upslope movements totaling up to 150 m. We will come back to this in the discussion.

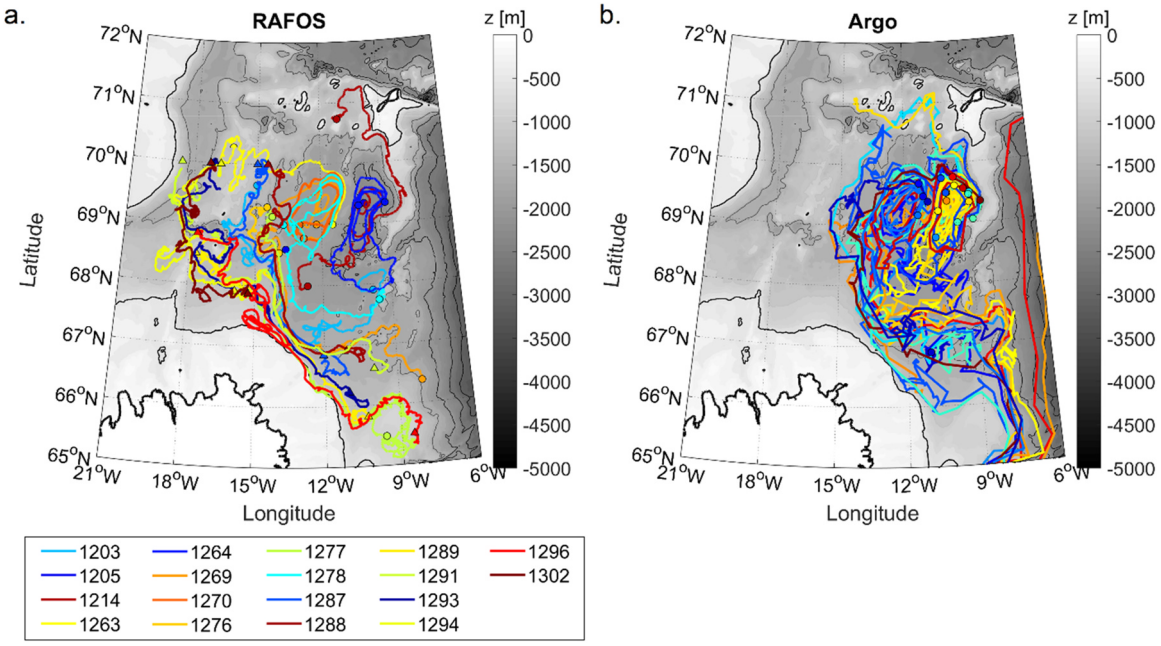

Fig. 4. Tracks of RAFOS (a) and Argo (b) floats deployed in the deep Iceland Sea basin. a.) RAFOS trajectories in interior Iceland Basin and those released west of the Kolbeinsey Ridge that proceeded through the Spar Fracture Zone. Deployment positions are indicated with circles (triangles) for summer 2013 (2014). b.) 10-day displacement trajectories of 21 Argo floats in the Iceland Sea. Initial Argo positions are indicated by a circle in the same color as the track. The flow is composed of two cyclonic cells, centered at about 68°N, 12°W 68°N, 10°W, which seemed to be topographically steered. Isobaths are drawn in gray every 500 m and the 500 m isobath is drawn in black. (For interpretation of the references to color in this figure legend, the reader is referred to the web version of this article.)

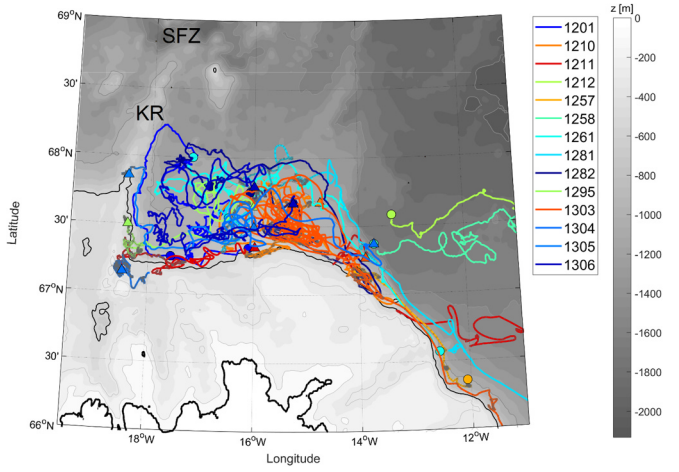

Fig. 5. Zoom in on tracks near the Icelandic shelf east of the KR. Triangles (circles) indicate tracks of floats released in 2013 (2014). Grounded parts of positions in tracks have been indicated in gray. The 500 m isobath in drawn in black.

3.3. Circulation west of the Kolbeinsey Ridge

All floats that were deployed in 2013 and 2014 west of the KR that remained west of the ridge are presented in Fig. 6a. In July 2013, three RAFOS floats were deployed on the Greenland slope just south of 70°N of which one (RF1262) was lost. The other floats (RF1260, RF1280) initially moved rapidly along the slope southward. RF1260 followed the slope tightly to about 69°N and then gradually moved away from the slope and after about 100 days it moved into mid channel. RF1280 on the other hand left the slope just south of 69°N and moved into the middle of the Blosseville Basin (BB). Eventually RF1280 drifted north and then on to the Iceland north slope, the same fate as RF1260. Both floats grounded and were pushed up slope along the bottom. Both shoaled by about 300 m and remained on the bottom for the remainder of their missions.

In July 2014, seven RAFOS floats were deployed on the Greenland slope close to 70°N, and three were deployed on the western slope of the Kolbeinsey Ridge in the BB (Fig. 6). Four of these floats (RF1208, RF1209, RF1297 and RF1301) exited the Iceland Sea to the Irminger Sea through Denmark Strait. Both RF1208 and 1209 were deployed close (130 m) to the bottom: both exited the Iceland Sea after about 110 days. However, their paths toward Denmark Strait were quite different. RF1208 left the Greenland slope just south of 69°N and crossed the BB and underwent some small scale eddy motion along the Iceland slope before exiting through Denmark Strait. RF1209 on the other hand followed the slope to 68°N. Due to limited acoustic signals we were not able to construct the trajectories all the way to the sill of the Denmark Strait. Instead, the crossing of the sill is determined from an abrupt increase in temperature and increase in pressure as the float settled into the hydrographic regime of the Irminger Sea. The fact that RF1208 and RF1209 crossed the sill at more or less the same time (about 110 days after deployment) indicated that RF1209 was subjected to eddy motion before it exited the Denmark Strait. If it had been advected directly to the strait it would have exited earlier than RF1208. RF1297, which was deployed close to RF1208 and RF1209, followed the Greenland slope and left the slope very close to RF1208, but it remained for a while in the deeper part of the BB before crossing over to the Iceland slope, and exited through Denmark Strait after about 300 days. RF1301, deployed at the bottom of the slope, was advected directly toward the Iceland slope and exits the Denmark Strait about 180 days after deployment. Of the remaining floats deployed on the Greenland slope, one returned to the surface early (RF1292), one (RF1293) drifted east through the Spar Fracture Zone and one (RF1298) moved over to the Icelandic slope west of the KR and grounded there.

More floats were deployed west of the Kolbeinsey Ridge near the Icelandic slope, three floats in 2013 and four in 2014 (Fig. 1). All three floats deployed in 2013 returned data. One float (RF1200) was deployed just to the west of the Spar Fracture Zone close to 69°N. This float drifted south and followed the KR and the north Icelandic slope before it moved westward and eventually crossed over to the Greenland

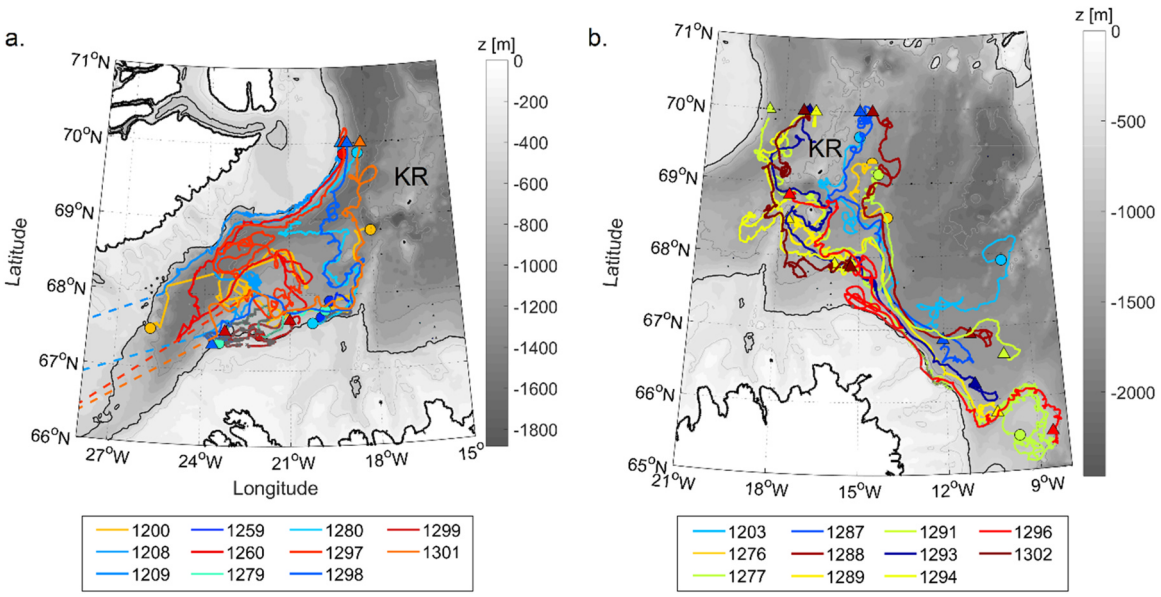

Fig. 6. Float tracks of RAFOS floats deployed at 70°N in the east and west of the Kolbeinsey Ridge (KR). a.) Floats that remained west of the KR. b.) The floats deployed in the channel and east of KR that followed the East Icelandic Current towards the Norwegian Sea. (Some tracks that were presented in Fig. 4, are presented here as well. The colors for each track are the same in both figures.) Grounded parts of positions in tracks have been indicated in gray. The 500 m isobath is drawn in black. (For interpretation of the references to color in this figure legend, the reader is referred to the web version of this article.)

slope where it surfaced just south of 68°N. The two floats (RF1259 and RF1279) deployed at the north slope of Iceland in 2013 both grounded after 10–20 days. Only one (RF1299) of the four floats deployed at the north Iceland slope in 2014 returned data, and this float grounded after only 5–10 days.

Thus, of the five floats that were deployed west of the Kolbeinsey Ridge in 2013 and returned data, four grounded on the north slope of Iceland. Due to a ballasting error these four floats had an equilibrium depth of 700–800 m and would not have been able to exit over the Denmark Strait sill. The remainder of the floats (six floats) discussed above all had equilibrium depth of 500–600 m. Only one of these floats (RF1298) grounded. Of the other five, four exited the Iceland Sea through Denmark Strait. It is also noteworthy that even though the several floats drifted very close to the bottom along the Greenland slope, none of the floats grounded, whereas a large fraction of the floats grounded on the north slope of Iceland indicating large cross slope flows.

Even though the floats along the northern slope of Iceland were generally at (or driven up to) shallower depths, the sensors registered lower temperatures. At 380 m depth on the slope the floats registered a temperature of − 0.4 °C, while slightly further offshore temperatures were around − 0.2 °C at 590 m depth (Fig. 7). This seems indicative of deeper, colder water being driven up the slope. Upwelling of colder water on the Icelandic slope is also visible in the standard Icelandic sections (Jónsson and Valdimarsson, 2004; Pickart et al., 2017).

3.4. Mesoscale and other small scale motions

The Iceland Sea is known as an area of low eddy kinetic energy (EKE) relative to other nearby basins (Jakobsen et al., 2003), such as the Lofoten eddy (Søiland et al., 2016) or the strong EKE region off southwest Greenland (de Jong et al., 2014, 2016). The results of the wavelet analysis of the float tracks give more insight into scales of coherent motions in the Iceland Sea. Sections of coherent swirling or cusping (both cyclonic and anti-cyclonic) were found in 19 of the 45 float tracks (Fig. 8), occasionally with multiple occurrence along different geographical section of the same track. In the central Iceland Sea the radii are small, between 0.2 and 3 km, low azimuthal velocities, between 0.5 and 3 cm s^{-1}. and small (~ 0.15) Rossby numbers. Eddies in the southwest, near the passage towards the Norwegian Sea, had

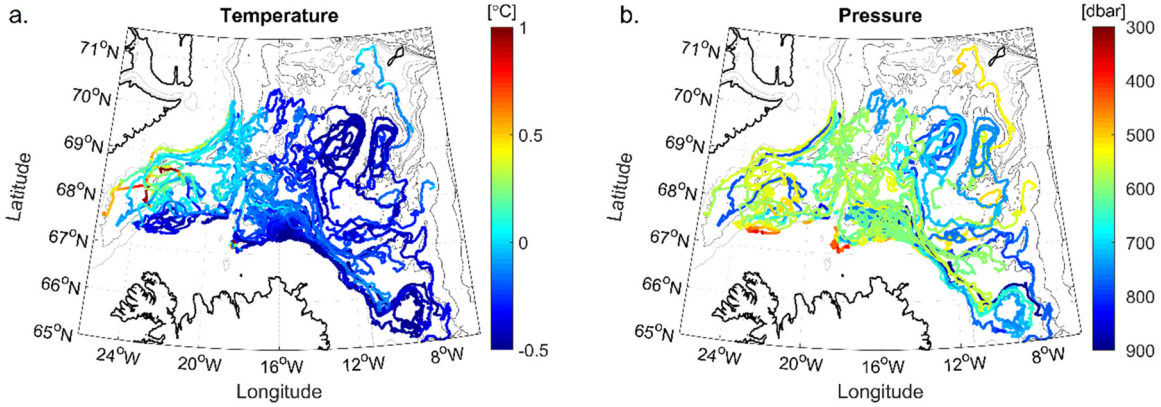

Fig. 7. Temperature (a) and pressure (b) along float tracks. This shows the warmer EGC water going southeastward through the Spar Fracture Zone and into the main basin. It also shows the colder water along the northern slope of Iceland caused by the local upward motions. Grounding, visible as pressures shallower then 400 dbar, mainly took place in these areas.

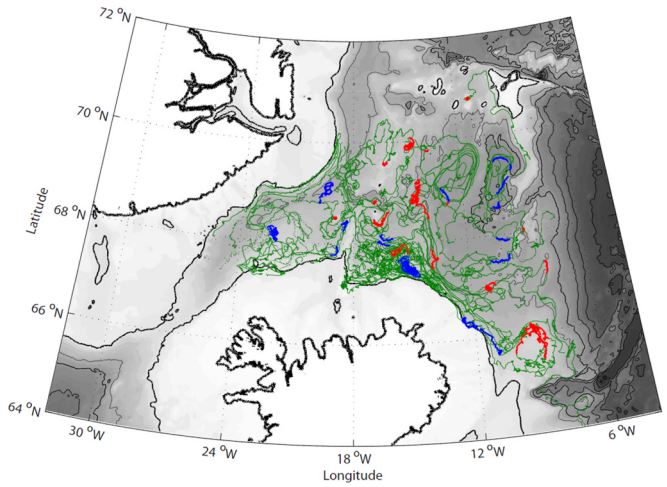

Fig. 8. Results of the eddy detection wavelet analysis. Original float tracks are drawn in green. Sections of float tracks identified as exhibiting coherent cyclonic (anticyclonic) behavior are drawn in blue (red). (For interpretation of the references to color in this figure legend, the reader is referred to the web version of this article.)

radii of about 3 km and velocities of 3–5 cm s^{-1}. In this area, where the EIC leaves the Iceland Sea, the coherent "boundary" eddies spin up inshore of the main boundary current and slope are similar to the type of anti-cyclonic eddies that were present in the Gulf of Mexico between the cyclonic boundary current and slope (Furey et al., 2018).

Overall, the Iceland Sea eddies are too small to stand out in altimetry. Largest azimuthal velocities (12 cm s^{-1}) were seen in RF1208 in the central BB around 68.5°N. The estimated radius and period of this cyclonic eddy are 3 km and 2–3 days. These values resemble measurement from mooring current meters in the same region. Harden and Pickart (2018) describe topographic waves (with a period of 3.6 days) upstream of Denmark Strait, which they suggest may be associated with the Separated East Greenland Current.

Along the EIC, from the SFZ to the region of accelerated flow at 14°W, both cyclonic and anti-cyclonic motions are found. Radii are in the same range as in the rest of the basin, 1–4 km. One (free floating) float, RF1303, deployed on the Langanes section, remained in the area near the slope between 16.5° and 14°W for 200 days before following the EIC southwestward. This float exhibited cyclonic motion, with approx. azimuthal velocities of 10 cm s^{-1}, starting with a radius of 2 km and increasing to 8 km and a Rossby number of 0.4 decreasing to 0.1. The small scale motions between the EIC and the north Icelandic slope were not identified as coherent motions by the wavelet analysis.

4. Discussion

The tracks of RAFOS floats deployed in summer of 2013 and 2014 elucidate the circulation of the Iceland Sea. These tracks highlight the slow, double gyre cyclonic circulation in the interior basin. They also show the strong eastward connection from the East Greenland Current towards the Norwegian Sea of which the first half (from EGC to Iceland Sea) had been shown by Macrander et al. (2014) and the second half (to the Norwegian Sea) by Voet et al. (2003). This feature, known as the East Icelandic Current, has traditionally been included in circulation schemes of the Iceland Sea (Stefánsson, 1962; Swift and Aagaard, 1981; Malmberg et al., 1996) but was only mentioned as a possible upper layer pathway through the Spar Fracture Zone in the revised circulation scheme of Våge et al. (2013). Macrander et al. (2014) mainly focused on the EIC above 170 m, on the shelf and partly over the NIJ, because of their interest in freshwater transport. However, their section also shows deep reaching southeastward velocities further offshore. The RAFOS tracks presented here show that this offshore branch of the EIC reaches at least 600 m deep, is joined by water from the interior basin, and continues southeastward along the northeast Icelandic slope towards the Norwegian Sea. The floats that surfaced near the Faroe Shetland Channel indicated the potential contribution of dense water from the EGC and Iceland Sea to the Faroe Bank Channel overflow, as do the Argo trajectories shown here, and help substantiate the pathway presented by Köhl (2010).

The EIC is likely a barrier against entrainment of water from the interior Iceland Sea into the NIJ, but part of the EIC water itself maybe entrained. Virtual particles tracked upstream by Behrens et al. (2017) in high resolution (1/20°) regional model showed a similar pathway providing about 15% of the overflow water. Contrary to our finding, Behrens et al. (2017) associated this pathway with downwellling water from the NIIC rather than connecting it with the flow of the EIC through the Spar Fracture Zone. They also found that part of the flow towards Denmark Strait on the northwest Icelandic slope derives from the EGC. An end member analysis in Denmark Strait by Mastropole et al. (2017) finds a high contribution of Arctic origin water (defined as from the central Iceland Sea) to the main overflow, but also an extension of this contribution to the west up the Greenland slope of Denmark Strait. We propose that both have the same source, the dense water in the deeper part of the EGC is partly entrainment into the water on the western slope and the similarly the diversion of this dense water from the EGC with the EIC into the Iceland Sea creates a high contribution on the Icelandic side. In this study, float tracks were diverted from the EGC towards the Icelandic slope west of the KR, where a ~ 25–30 cm s^{-1} flow directed towards the sill was seen, indicating at least a strong contribution from the EGC to the NIJ there.

A direct pathway connection between the interior Iceland Sea and the Denmark Strait overflow was not found in this study. Some floats deployed in the Langanes section, around 67°N and 14°W, showed westward flow towards the KR, but they turn back east as they encounter the EIC near the Spar Fracture Zone. The region between the Kolbeinsey Ridge and the acceleration of the southeastward flow off the steep Icelandic slope at 14°W is very rich in apparently non-coherent small scale motions. Floats deployed in this area had a relative high residence time and eventually either joined the EIC or were driven up several hundred meters on the Iceland slope. Whether the nature of the floats, being isobaric rather than isopycnal, was a factor in the grounding of the floats is not clear. Several of the floats deployed in the EGC at 70°N faced a similar fate on the Icelandic slope west of the KR.

The RAFOS floats are equipped to transmit pressure and temperature data measured at 15-min intervals, and from these higher-resolution data, we were able to calculate vertical velocities derived from float displacements. We found short term (15-min period) velocities of up to ± 4 cm s^{-1} and during up slope events vertical velocities up to 0.15 cm s^{-1} over a 4 h period. During these events the floats were in contact with the bottom and thus not represent the true vertical velocities. Even so, they are quite large compared to the horizontal velocities offshore (~ 10 cm s^{-1}). The upward motion of deeper water north of Iceland on both sides of the KR results in a narrow rim of lower temperatures. Jónsson and Valdimarsson (2004) suggested that the colder water on the Icelandic slope may be the result of a bottom Ekman layer generated by the North Icelandic Jet. Pickart et al. (2017) suggest that it may be a compensating mechanisms for offshore flow observed in the upper layers when the inshore front of the NIJ is collocated with the offshore front of the NIIC. However, the exact mechanisms of the upslope motion needs further study.

It is surprising that the float tracks did not elucidate a NIJ pathway around the Kolbeinsey Ridge. Floats deployed in this region generally started at pressures between 539 and 613 dbar (with the exception of a few over ballasted floats in the first year due to the incorrect TEC). These pressures should have enabled them to be entrained into the NIJ, which can extend down to 800 m (Pickart et al., 2017). In fact, the floats did encounter the cold upwelling water associated with the NIJ. Why these floats were moved upslope rather than being advected

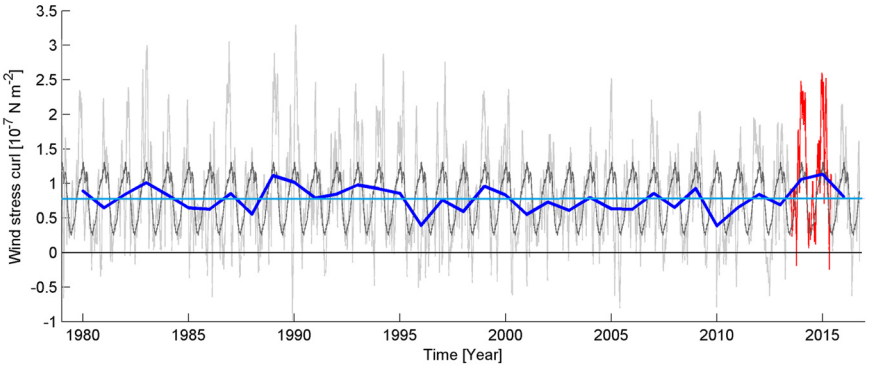

Fig. 9. Time series of wind stress curl over the area around Iceland (60°N, 40°W; 72°N, 10°W; 60°N, 10°W) positively correlated with overflow transport in the study by Köhl et al. (2007). The daily wind stress curl over the whole record is drawn in light gray and over the RAFOS experiment period in red. The mean seasonal cycle is drawn in dark gray and annual average values (from 1 June to 31 May) are drawn with the thick darker blue line. The lighter blue horizontal line indicates the overall mean value of the wind stress curl. (For interpretation of the references to color in this figure legend, the reader is referred to the web version of this article.)

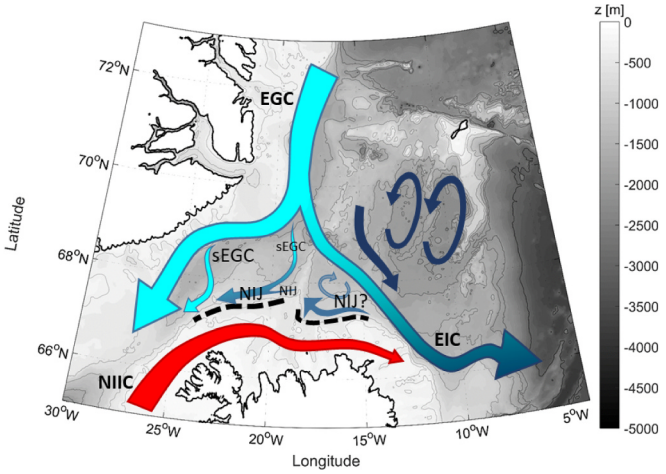

Fig. 10. Current schematic incorporating the information from this float experiment into previously published schematics. Areas of upslope motion are indicated with the thick dashed black lines. Indicated currents are East Greenland Current (EGC), Separated East Greenland Current (sEGC), North Icelandic Irminger Current (NIIC), North Icelandic Jet (NIJ) and the East Icelandic Current (EIC).

horizontally from east to west of the KR will need to be studied further.

The atmospheric forcing conditions during the experiment may have also attributed to the lack of a clear NIJ pathway in the float tracks. In a model study, Köhl (2010) found that the sources of dense water at the Denmark Strait sill depended on the wind forcing around Iceland. During moderately strong wind stress curl conditions around Iceland the model's EGC was found to be the main source to the Denmark Strait overflow. In this case the Iceland Sea circulation was found to strengthen and entrain water from the EGC and NIIC. During weak wind stress curl conditions the interior circulation relaxes and the Iceland Sea becomes a source to the Denmark Strait overflow. To investigate wind stress curl conditions during the float observational time period, we produced a time series of wind stress curl over the area around Iceland identified by Köhl et al. (2007) as having a positive correlation with barotropic transport through Denmark Strait (approx. between 60°N, 40°W; 60°N, 10°W and 72°N, 10°W), from the ERA Interim reanalysis data. The time series of ERA Interim wind stress curl averaged over this region (Fig. 9) shows that the wind stress curl was strong during the 2013–2015 float experiment period. This would favor a strong connection with the EGC rather than a strong westward NIJ. According to the linkages suggested by Köhl et al. (2007), the wind stress conditions were more favorable for a strong NIJ in 2001 AND 2002, the years described by Jónsson and Valdimarsson (2004), as well as during 2008 and 2009, the years described by Våge et al. (2011).

The pathways of the RAFOS floats deployed in this experiment showed the strong connection between the East Greenland Current and the Norwegian Sea, via de East Icelandic Current, which already appeared in early flow schematics (Swift and Aagaard, 1981). The float tracks also show a clear connection between the EGC and the NIJ west of the KR. Both of these features are not clearly represented in the current schematic that has been published by Våge et al. (2013). The pathway associated with the Separated EGC (sEGC) was also shown by the floats, however it remains unclear whether the sEGC is a current or consists of intermittent current branches or eddies. Therefore we have drawn a new schematic (Fig. 10), based on Våge et al. (2013) and the new information from this float experiment. Two features in this map remain a subject of investigation; the eastern source of the NIJ, and the nature of the Separated EGC (sEGC).

Acknowledgements

This work was supported by US National Science Foundation Grant OCE- 1259210 and the Bjerknes Center for Climate Research. Institute of Marine Research provided shiptime for the three deployment and recovery cruises. We thank the captain and crew of the R/V Håkon Mosby for the assistance on successful cruises.

MFdJ provided half of the floats for this project, analyzed float data, prepared the figures and wrote most of the paper. HS conceived the project, planned the fieldwork, provided and ballasted the half of the floats, and provided and deployed the sound sources for tracking. AB oversaw preparation and ballasting of the floats. HF processed and tracked the float data.

References

Behrens, E., Våge, K., Harden, B., Biastoch, A., Böning, C.W., 2017. Composition and variability of the Denmark Strait overflow water in a high-resolution numerical model hindcast simulation. J. Geophys. Res. Oceans 122, 2830–2846. https://doi.org/10.1002/2016JC012158.

Bower, A.S., Hendry, R.M., Amrhein, D.E., Lilly, J.M., 2013. Direct observations of formation and propagation of subpolar eddies into the Subtropical North Atlantic. Deep Sea Res. II 85, 15–41. https://doi.org/10.1016/j.dsr2.2012.07.029.

Furey, H., Bower, A., Perez-Brunius, P., Hamilton, P., Leben, R., 2018. Deep eddies in the Gulf of Mexico observed with floats. J. Phys. Oceanogr (In review).

Gill, A.E., 1982. Atmosphere-ocean dynamics. International Geophysics Series. Academic Press, London, pp. 22–38.

Harden, B.E., Pickart, R.S., 2018. High-frequency variability in the North Icelandic jet. J. Mar. Res (Accepted in Journal of Marine Research).

Harden, B.E., Pickart, R.S., Valdimarsson, H., Våge, K., de Steur, L., Richards, C., Bahr, F., Torres, D., Børve, E., Jónsson, S., Macrander, A., Østerhusg, S., Håvik, L., Hattermann, T., 2016. Upstream sources of the Denmark strait overflow: observations from a high-resolution mooring array. Deep-Sea Res. I 112, 94–112.

Helland-Hansen, B., Nansen, F., 1909. The Norwegian Sea. its physical oceanography based upon the Norwegian researches 1900–1904. Report. Nor. Fish. Mar. Investig. 2 (2), 390 (Pt. I).

de Jong, M.F., Bower, A.S., Furey, H.H., 2016. Seasonal and inter-annual variations of Irminger Ring formation and boundary-interior heat exchange in FLAME. J. Phys. Oceanogr. https://doi.org/10.1175/JPO-D-15-0124.1.

Jakobsen, P.K., Ribersgaard, M.H., Quadfasel, D., Schmith, T., Hughes, C.W., 2003. The near-surface circulation in the northern North Atlantic as inferred from drifter data: variability from the mesoscale to interannual. J. Geophys. Res. 108. https://doi.org/10.1029/2002JC001554.

de Jong, M.F., Bower, A.S., Furey, H.H., 2014. Two years of observations of warm core anticyclones in the Labrador Sea and their seasonal cycle in heat and salt stratification. J. Phys. Oceanogr. 44, 427–444. https://doi.org/10.1175/jpo-d-13-070.1.

Jeansson, E., Jutterström, S., Rudels, B., Anderson, L.G., Olsson, K.A., Jones, E.P., Smethie, W.M., Swift, J.H., 2008. Sources to the East Greenland Current and its contribution to the Denmark Strait Overflow. Prog. Oceanogr. 78, 12–28. https://doi.org/10.1016/j.pocean.2007.08.031.

Jochumsen, K., Moritz, M., Nunes, N., Quadfasel, D., Larsen, K.M.H., Hansen, B., Valdimarsson, H., Jonsson, S., 2017. Revised transport estimates of the Denmark Strait overflow. J. Geophys. Res. Oceans 122, 3434–3450. https://doi.org/10.1002/2017JC012803.

Jónsson, S., Valdimarsson, H., 2004. A new path for the Denmark Strait overflow water from the Iceland Sea to Denmark Strait. Geophys. Res. Lett. 31, L03305 (doi:10/1029/2003GL01924).

Jónsson, S., 1999.The circulation in the northern part of the Denmark Strait and its variability. ICES Report CM-1999/L:06, p. 9.

Köhl, A., 2010. Variable source regions of Denmark Strait and Faroe Bank Channel overflow waters. Tellus A 62, 551–568.

Köhl, A., Käse, R.H., Stammer, D.B., 2007. Causes of changes in the Denmark Strait overflow. J. Phys. Oceanogr. 37, 1678–1696.

Latarius, K., Quadfasel, D., 2016. Water mass transformation in the deep basins of the Nordic Seas: analyses of heat and freshwater budgets. Deep Sea Res. Part I: Oceanogr. Res. Paper 114, 23–42. https://doi.org/10.1016/j.dsr.2016.04.012.

Lilly, J.M., Gascard, J.-C., 2006. Wavelet ridge diagnosis of time-varying elliptical signals with application to an oceanic eddy. Nonlinear Process. Geophys. 13, 467–483.

Lilly, J.M., Olhede, S.C., 2009a. Higher-order properties of analytic wavelets. IEEE Trans. Signal Process. 57, 146–160.

Lilly, J.M., Olhede, S.C., 2009b. Wavelet ridge estimation of jointly modulated multivariate oscillations. In: Proceedings of the 43rd Asilomar Conference on Signals, Systems, and Computers, pp. 452–456. Refereed Conference Proceedings paper.

Lilly, J.M., Olhede, S.C., 2010a. Bivariate instantaneous frequency and bandwidth. IEEE Trans. Signal Process. 58, 591–603.

Lilly, J.M., Olhede, S.C., 2010b. On the analytic wavelet transform. IEEE Trans. Inf. Theory 56 (8), 4135–4156.

Lilly, J.M., Olhede, S.C., 2012. Analysis of modulated multivariate oscillations. IEEE Trans. Signal Process 60 (2), 600–612.

Logemann, K., Ólafsson, J., Snorrason, Á., Valdimarsson, H., Marteinsdóttir, G., 2013a. The circulation of Icelandic waters – a modelling study. Ocean Sci. 9, 931–955. https://doi.org/10.5194/os-9-931-2013.

Logemann, K., Ólafsson, J., Snorrason, Á., Valdimarsson, H., Marteinsdóttir, G., 2013b. The circulation of Icelandic waters – a modelling study. Ocean Sci. 9, 931–955. https://doi.org/10.5194/os-9-931-2013.

Macrander, A., Valdimarsson, H., Jónsson, S., 2014. Improved transport estimate of the East Icelandic Current 2002–2012. J. Geophys. Res. Oceans 119, 3407–3424. https://doi.org/10.1002/2013JC009517.

Malmberg, S.-A., Valdimasson, H., Mortensen, J., 1996. Long-time series in Icelandic waters in relation to physical variability in the northern North Atlantic. NAFO Sci. Counc. Stud. 24, 69–80.

Mastropole, D., Pickart, R.S., Valdimarsson, H., Våge, K., Jochumsen, K., Girton, J., 2017. On the hydrography of Denmark Strait. J. Geophys. Res. Oceans 122, 306–321. https://doi.org/10.1002/2016JC012007.

Mauritzen, C., 1996. Production of dense overflow waters feeding the North Atlantic across the Greenland-Scotland Ridge. 1. Evidence for a revised circulation scheme. Deep Sea Res. I 43, 769–806.

Pickart, R.S., Spall, M.A., Torres, D.J., Våge, K., Valdimarsson, H., Nobre, C., Moore, G.W.K., Jonsson, S., Mastropole, D., 2017. The North Icelandic Jet and its relationship to the North Icelandic Irminger current. J. Mar. Res. 75, 605–639.

Rossby, T., Dorson, D., Fontaine, J., 1986. The RAFOS system. J. Atmos. Ocean. Technol. 3, 672–679.

Rossby, T., Prater, M.D., Søiland, H., 2009. Pathways of inflow and dispersion if warm waters in the Nordic Seas. J. Geophys. Res. 114. https://doi.org/10.1029/2008JC005073.

Rudels, B., Fahrbach, E., Meincke, J., Budéus, G., Eriksson, P., 2002a. The East Greenland Current and its contribution to the Denmark Strait overflow. ICES J. Mar. Sci. 59, 1133–1154.

Rudels, B., Fahrbach, E., Meincke, J., Budéus, G., Eriksson, P., 2002b. The East Greenland Current and its contribution to the Denmark Strait overflow. ICES J. Mar. Sci. 59, 1133–1154.

Rudels, B., Eriksson, P., Buch, E., Budéus, G., Fahrbach, E., Malmberg, S.-A., Meincke, J., Mälkki, P., 2003. Temporal switching between sources of the Denmark Strait overflow water. ICES Mar. Sci. Symp. 219, 319–325.

Smethie, W.M., Swift, J.H., 1989. The tritium: krypton-85 age of Denmark Strait overflow water and gibbs fracture zone water just south of Denmark Strait. J. Geophys. Res. 94 (C6), 8265–8275.

Søiland, H., Prater, M.D., Rossby, T., 2008. Rigid topographic control of currents in the Nordic Seas. Geophys. Res. Lett. 35, L18607. https://doi.org/10.1029/2008GL034846.

Søiland, H., Chafik, L., Rossby, T., 2016. On the long-term stability of the Lofoten Basin Eddy. J. Geophys. Res. Oceans 121, 4438–4449. https://doi.org/10.1002/2016JC011726.

Stefánsson, U., 1962. North Icelandic waters. Rit Fiskid. 3, 269.

Swift, J.H., Aagaard, K., 1981. Seasonal transitions and water mass formation in the Iceland and Greenland seas. Deep Sea Res. Part A 28 (10), 1107–1129. https://doi.org/10.1016/0198-0149(81)90050-9.

Swift, J.H., Aagaard, K., Malmberg, S.-A., 1980. The contribution of the Denmark Strait overflow to the deep North Atlantic. Deep-Sea Res. 27A, 29–42.

Våge, K., Pickart, R.S., Spall, M.A., Valdimasson, H., Jónsson, S., Torres, D.J., Østerhus, S., Eldevik, T., 2011. Significant role of the North Icelandic Jet in the formation of Denmark Strait Overflow Water. Nat. Geosci. 4, 723–727.

Våge, K., Pickart, R.S., Spall, M.A., Moore, G.W.K., Valdimarsson, H., Torres, D.J., Erofeeva, S.Y., Nilsen, J.E.Ø., 2013. Revised circulation scheme north of the Denmark Strait. Deep-Sea Res. I 79, 20–39. https://doi.org/10.1016/j.dsr.2013.05.00.

Voet, G., Quadfasel, D., Mork, K.A., Søiland, H., 2003. The mid-depth circulation of the Nordic Seas derived from profiling float observations. Tellus A 62 (4), 516–529. https://doi.org/10.1111/j.1600-0870.2010.00444.x. (2010).